

Experimental Observation of Fluidlike Motion of Optical Vortices

D. Rozas, Z. S. Sacks, and G. A. Swartzlander, Jr.

Physics Department, Worcester Polytechnic Institute, Worcester, Massachusetts 01609

(Received 21 July 1997)

We have observed the fluidlike rotation of a pair of identical optical vortices (OV's) as they propagate through free space. Similar to vortex filaments in a fluid, the initial rotation rate is found to be inversely proportional to the squared distance of separation. Owing to unusually small vortex cores, we obtained rotation rates that were 2 orders of magnitude larger than expected for "conventional" large core OV's. [S0031-9007(97)04388-3]

PACS numbers: 42.25.-p, 42.40.Jv, 47.15.Ki, 47.32.Cc

It is well known that two identical vortex filaments in an incompressible inviscid fluid orbit each other at a rate inversely proportional to the orbital area [1] owing to an effective interaction manifested in the flow field. On the other hand, it has been shown analytically [2] and experimentally [3] that *optical vortices* (OV's) in a propagating beam having a Gaussian intensity profile exhibit rotation rates that are independent of the separation distance. This contrast seems to suggest that fluidlike effective interactions between OV's do not occur. However, both fluid flow and the diffraction of light may be described using potential theory, and one may expect similar phenomena to occur in both systems. Here we report the first experimental evidence of an effective interaction between identical OV filaments, showing that over short propagation distances (i.e., before the vortices diffract and overlap), the rotation rate indeed varies inversely with the squared distance of separation.

A topological vortex [4] in optics is characterized by a helical wave front and a dark circular core whose wave function vanishes at the central point owing to destructive interference. The electric field of a beam containing a single vortex may be expressed as

$$E(r, \phi, z) = E_{BG}(r, z)A(r, z) \exp[i\Phi(r, z)] \times \exp(-ikz) \exp(im\phi), \quad (1)$$

where E is the normalized scalar electric field, the background field is typically a Gaussian envelope $E_{BG}(r, z = 0) = \exp(-r^2/w_0^2)$ of size w_0 , and where (r, ϕ) are the polar coordinates in the transverse plane of the beam, Φ represents the wave front curvature of the propagating beam, z is the optical axis, $k = 2\pi/\lambda$ is the wave number, λ is the wavelength of light, and m is the topological charge. (Note that in quantum mechanics, m is an orbital angular momentum quantum number.) Finally, $A(r, z)$ is the core function describing the amplitude of the vortex core which vanishes at $r = 0$. We are primarily interested in so-called vortex filaments (or quasi-point vortices) which are characterized by a vanishing core size in the initial plane. A model function which has a well-defined core size w_V arises in various physical systems (such as nonlinear refractive media [5–7] and Bose-Einstein quantum

fluids [8]) and is given by

$$A(r, z = 0) = \tanh(r/w_V). \quad (2)$$

A point vortex exists in the theoretical limit as $w_V \rightarrow 0$, although it is not physical because the beam would contain infinite transverse momentum. The paraxial approximation will be assumed through this report so that, in practice, $w_0 \gg w_V \gg \lambda$.

Let us consider the propagation dynamics of a beam containing vortices as it evolves along the optical axis in the laboratory reference frame, rather than as a function of time in the frame moving at the speed of light. A fluidlike description of the "flow" of photons may be heuristically understood using a ray optics model. (This approach is justified for the initial propagation of point vortices on a uniform background field, because the beam contains only phase information [9].) It is well known that rays of light travel perpendicular to the wave front, which, for a single vortex, is described by the surface: $m\phi - kz + \Phi = \text{const}$. The negative gradient of this surface determines the ray directions, whose transverse components are given by the transverse wave vector

$$\mathbf{k}_\perp = -\nabla_\perp[m\phi - kz + \Phi(r, z)] = -\hat{r}\partial\Phi/\partial r - \hat{\phi}m/r, \quad (r \neq 0), \quad (3)$$

where \hat{r} and $\hat{\phi}$ are radial and azimuthal unit vectors, respectively. For paraxial rays, the important azimuthal component $\mathbf{k}_\phi = -\hat{\phi}m/r$ must vanish at the origin [10]. The effect of the vortex factor in Eq. (1), $\exp(im\phi)$, is evident in Eq. (3), namely, it provides an angular component to all the ray trajectories.

Fluid flow about a vortex, on the other hand, may be described with two-dimensional potential theory where the expression $m\phi$ has the meaning of a potential, its negative gradient, $-\nabla_\perp(m\phi)$ is the flow velocity, and the azimuthal velocity is thus proportional to $1/r$ [11]. By comparison, one may therefore surmise that \mathbf{k}_\perp is analogous to the velocity field of an ideal fluid, and that a pencil of light rays may circumnavigate the optical vortex core as the beam propagates through space just as molecules in a fluid circle about the core of a vortex. In the latter case, we note that

a particle at the *center* of a given vortex core is unaffected by the flow established by that vortex.

To test this analogy, a second vortex may be placed in the beam. As in a fluid, the flow established by the first vortex is expected to transport the second vortex (and vice versa), resulting in an effective vortex-vortex interaction. When multiple vortices exist in the same beam, the initial field may be written as a series of products:

$$E(r, \phi, z = 0) = E_{BG}(r) \prod_{j=1}^M A_j(r_j) \exp(im_j \phi_j), \quad (4)$$

where the j th vortex is characterized by a core function A_j , a topological charge $m_j = \pm 1$, and circular coordinates (r_j, ϕ_j) , defined at each core as shown in Fig. 1. (A different class of experiments may be conducted by, instead, superimposing vortex fields [12].) For convenience, we assume an initially flat wave front curvature $\Phi(r, z = 0) = 0$. From an experimental point of view, vortices may be introduced using one or more phase masks. In our experiment, we consider two identical singly charged vortices ($M = 2$, $m_1 = m_2 = 1$, $A_1 = A_2$), separated by a distance $d_V \ll w_0$, and placed at the center of the beam, as depicted in Fig. 1. In the near field region $|z| \ll z_V$ where

$$z_V \equiv \pi d_V^2 / \lambda \quad (5)$$

characterizes the distance at which the vortex cores overlap owing to diffraction, the effects of diffraction may be ignored, and the field for a pair of point vortices may be written as $E(r, \phi, z) \equiv \exp[i(\phi_1 + \phi_2) - ikz]$. The initial phasefront for this field is shown in Fig. 1(b), depicting a circular phase ramp from 0 to 2π around each vortex. In this case, the net transverse wave vector may be expressed as

$$\mathbf{k}_\perp = -\hat{\phi}_1/r_1 - \hat{\phi}_2/r_2, \quad (6)$$

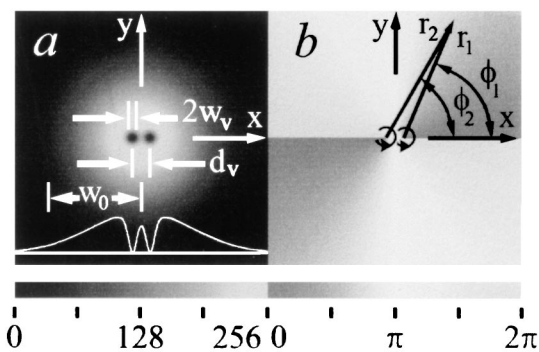


FIG. 1. (a) Intensity (log gray scale) and (b) phase (linear gray scale) profiles depicting two vortices of radial size w_V and separation d_V in the cross section of a Gaussian beam of size w_0 . The topological charge for each vortex is $m = 1$, resulting in a counter-clockwise circulation, as depicted by the circular arrows in (b). A line plot of the intensity along the x axis is shown in (a).

where $\hat{\phi}_1$ and $\hat{\phi}_2$ are unit vectors along the azimuth of each vortex. The mutual effective interaction between the OV's may now be described. The center of vortex 2 has an azimuthal component $\mathbf{k}_\perp(r_2 = 0) = -\hat{\phi}_1/d_V$, and vortex 1 has $\mathbf{k}_\perp(r_1 = 0) = -\hat{\phi}_2/d_V$. In other words, *vortex 2* is transported by the *phase gradient of vortex 1*, and vice versa. This suggests a double helical trajectory of the vortex cores as they propagate through space. The initial rotation rate, or angular “velocity” about a point midway between the vortices may thus be calculated [9,13]:

$$\Omega_V = \Delta\theta_V/\Delta z = -\lambda/\pi d_V^2 = -1/z_V, \quad (7)$$

where $\Delta\theta_V$ is the angular displacement of the vortices from their initial position. Diffraction may be expected to significantly affect this rate after a propagation distance $\Delta z \approx z_V$, and thus, Eq. (7) accounts for rotation angles up to roughly one radian. Thus we believe the analogy between optical and hydrodynamic vortex filaments is justified over short propagation distances.

In contrast, conventional optical vortices [14,15] have a core function $A_j(r_j) = r_j/L$, where L is a parameter characterizing the slope of the vortex core, but *not* the size; rather, the size is on the order of the background beam size. The propagation dynamics for such a large core function is significantly different from that of a quasi-point vortex. For an arbitrary number and placement of identical conventional vortices on a Gaussian background field, the rotation rate depends only on the size of the background beam

$$\Omega_G = -d\theta_G/dz = -[1 + (z/z_0)^2]^{-1} z_0^{-1}, \quad (8)$$

where $z_0 = \pi w_0^2/\lambda$ is the characteristic diffraction length of the Gaussian background beam, and $\theta_G(z) = \arctan(z/z_0)$. In contrast, the angular velocity for a point vortex pair may initially be many orders of magnitude larger than Eq. (8)—by a factor of $\Omega_V/\Omega_G = z_0/z_V = (w_0/d_V)^2$, assuming $d_V \ll w_0$. What is more, we point out that conventional vortices do not exhibit circular motion, but rather parallel rectilinear motion [9], owing to a z dependence of the separation distance. By induction, we conclude that only small core OV's exhibit fluidlike propagation dynamics.

To investigate the spiral trajectory of optical vortex filaments, we produced computer-generated holograms [16] of two small-core vortices. Holograms having a grating period of $120 \mu\text{m}$ were recorded onto acetate using a Linotronic laser printer with a 5080 dot/inch resolution. The holographic image of the vortex pair was initially reconstructed with a 34 mm diameter collimated single frequency argon ion laser beam of wavelength $\lambda = 514 \text{ nm}$. The first order diffracted beam containing the vortex pair was spatially filtered with a 310 mm focal length achromatic lens L_1 , and a $400 \mu\text{m}$ diameter pinhole P, as shown in Fig. 2. A second lens L_2 of focal length

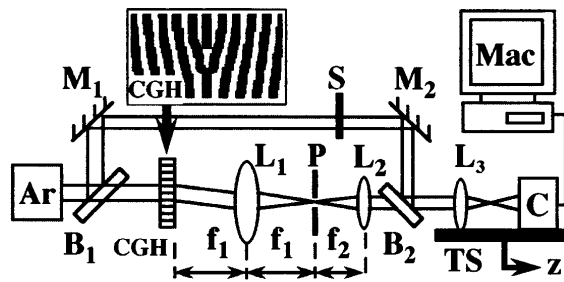


FIG. 2. Experimental setup: Ar: single frequency argon ion laser ($\lambda = 514$ nm); $B_{1,2}$: beam splitters; C: CCD camera; CGH: computer generated hologram (inset shows central region) with incident collimated beam of diameter 34 mm; $L_{1,2}$: lenses with focal lengths, $f_1 = 310$ mm, $f_2 = 63$ mm, respectively; L_3 : microscope objective (NA = 0.25); $M_{1,2}$: mirrors; Mac: Macintosh IIfx computer and framegrabber; P: 400 μm diameter pinhole; S: shutter; TS: translation stage aligned with the optical axis z .

63 mm, was used to re-collimate and reduce the beam to a size $w_0 = 3.5$ mm. In the image plane (where we set $z = 0$), we measured the vortex size to be $w_V \approx 60$ μm . The vortex separation distance was measured to range from $d_V \approx 100$ to 250 μm for different holograms. For the cases $d_V > 120$ μm the pair of vortex cores did not significantly overlap; i.e., they satisfied the quasipoint vortex condition $2w_V < d_V \ll w_0$.

Cross-sectional intensity profiles were recorded at various propagation distances [see, for example, Fig. 3(a)–3(c)] by translating an assembly containing a microscope objective L_3 and a CCD camera. The corresponding interferograms, shown in Fig. 3(d)–3(f) and displaying the unique forking pattern of two singly charged vortices, were obtained by opening a shutter S along the reference arm of a Mach-Zehnder interferometer. Relative positions of the vortices were obtained from the recorded profiles, which allowed us to determine the angular position θ_V and the separation distance at various propagation distances z from the image plane. By roughly aligning the axis of

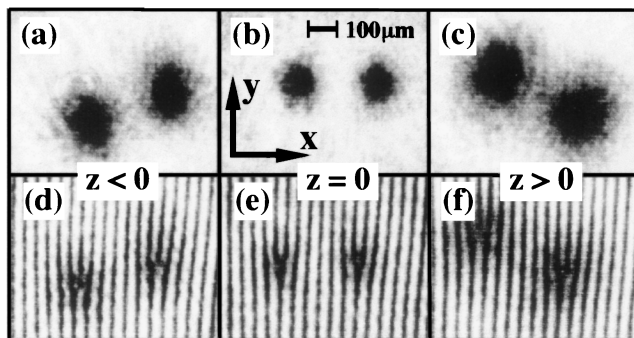


FIG. 3. Intensity (a)–(c) and interference (d)–(f) profiles of vortices of initial size $w_V \approx 60$ μm at different propagation distances (camera view). The vortices rotate clockwise for increasing values of z , as expected for positive topological charges.

the translation stage with the optical axis of the beam, the vortices appeared to move about a common axis, although measurements of the absolute positions of the vortices would be needed to verify this.

Initial rotation rates at $z = 0$, shown in Fig. 4(a), are in good agreement with the values predicted by Eq. (7) for $d_V > 2w_V$, as expected. An example of the varying rotation angle for the case $d_V = 105 \pm 9$ μm is plotted in Fig. 4(b), which shows a peak rotation at $z \approx z_V = 6.7$ cm, and rotation angles spanning 40° over a range of 11 cm. The relative vortex trajectories shown in Fig. 4(c) for three different values of d_V , indicate that the initial orbital motion of the vortex cores is followed by a repulsion from the center. The peak rotation angles experienced in these cases were 2 orders of magnitude larger than the angular position θ_G for conventional vortices, and thus, the observed effect may be solely attributed to the effective vortex-vortex interaction.

The departure from circular motion seen in Fig. 4(c), and the decelerated rotation rate seen in Fig. 4(b), is attributed to radiation from the diffracting vortex cores for $|z| > z_V$. The surprising decrease in the value of $|\theta_V|$ after reaching a peak value, as seen in Fig. 4(b), may be understood by considering the effect of the amplitude gradient on the vortex trajectory. Once the vortex cores begin

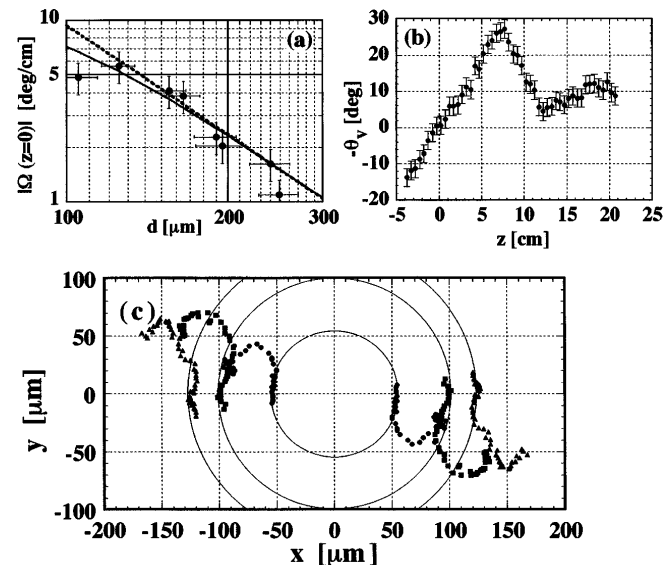


FIG. 4. (a) Experimental (points) and theoretical (curves) initial rotation rates, $|\Omega(z=0)| = |d\theta_V/dz|_{z=0}$, as a function of separation distance d_V . The dashed line represents the rate for point vortices [from Eq. (7)], while the gray curve is predicted from Eq. (9), assuming $w_V = 60$ μm . (b) Angular position of a vortex undergoing pairwise rotation as a function of propagation distance z for an initial vortex separation distance $d_V = 105 \pm 9$ μm ($z_V = 67$ mm). The orbit is initially clockwise [$(\Omega_V(z=0) < 0)$]. (c) Trajectories of vortex pairs in the transverse plane for initial separation distances d_V of 105 ± 9 μm (circles), 195 ± 17 μm (squares), 249 ± 21 μm (triangles). A common axis of motion has been assumed for the data.

to overlap [9], the nonuniform background field affects the vortex motion, and the rotation rate is estimated by

$$\Omega_{\tanh} \approx -(\lambda/\pi) \{d_V^{-2} + w_0^{-2} - 2/[d_V w_V \sinh(2d_V/w_V)]\}. \quad (9)$$

The vortex size w_V increases with propagation distance owing to diffraction, and thus, Eq. (9) accounts for a decrease in the rotation rate in the vicinity of $|z| \approx z_V$. To obtain accurate results, however, numerical solutions of the scalar diffraction equation are necessary. On the other hand, the effects of diffraction may be avoided by propagating beam through a self-defocusing nonlinear refractive medium, where the vortices propagate as optical vortex solitons [5]. In the latter case, numerical solutions [9] demonstrate that rotation angles exceeding 2π may be achieved.

In summary, small-core optical vortices having the same topological charge were found to rotate at an initial rate that increases inversely with the squared distance of separation. This phenomenon is analogous to the rotation of point vortices in a fluid. Furthermore, the initially large rotation rate, which was 2 orders of magnitude larger than predicted for conventional optical vortices, was observed to decrease and even reverse sign once the vortex cores overlapped. Control over the initial conditions provided by computer generated holography and high resolution laser printer technology makes the observation of this linear optical effect possible, and opens rich opportunities to explore other topological vortex phenomena such as turbulence and chaos [17] using linear and nonlinear optics as a testing ground.

We acknowledge insightful discussions with R. Y. Chiao (University of California, Berkeley) and C. T. Law (University of Wisconsin, Milwaukee), and the laboratory assistance of R. Shivitz (WPI). We are grateful to L. M. Narducci (Drexel University, Philadelphia), M. S. Soskin (Institute of Physics, Kiev), and A. Walther (WPI) for technical comments. G. A. Swartzlander was supported by the Research Corporation as a Cottrell Scholar and by the National Science Foundation as a Young Investigator. This work was also supported by Spectra-Physics Lasers,

Inc., and the Newport Corporation.

- [1] P. M. Morse and H. Feshbach, *Methods of Theoretical Physics* (McGraw-Hill, New York, 1953), Part II.
- [2] G. Indebetouw, *J. Mod. Opt.* **40**, 73–87 (1993).
- [3] I. V. Basistiy, V. Yu. Bazhenov, M. S. Soskin, and M. V. Vasnetsov, *Opt. Commun.* **103**, 422–428 (1993).
- [4] J. F. Nye and M. V. Berry, *Proc. R. Soc. London A* **336**, 165–190 (1974); M. Berry, in *Physics of Defects*, Proceedings of the Les Houches Summer School, Session XXXV, edited by R. Balian *et al.* (North-Holland, Amsterdam, 1981).
- [5] G. A. Swartzlander, Jr. and C. T. Law, *Phys. Rev. Lett.* **69**, 2503–2506 (1992).
- [6] R. Y. Chiao, I. H. Deutsch, J. C. Garrison, and E. M. Wright, *Serge Akhmanov: a Memorial Volume*, edited by H. Walther (Adam Hilger, Bristol, 1992).
- [7] A. W. Snyder, L. Poladian, and D. J. Mitchell, *Opt. Lett.* **17**, 789–791 (1992).
- [8] P. G. de Gennes, *Superconductivity of Metals and Alloys* (Addison-Wesley, New York, 1989), pp. 177–182.
- [9] D. Rozas, C. T. Law, and G. A. Swartzlander, Jr., *J. Opt. Soc. Am. B* **14**, 3049–3060 (1997).
- [10] The mean value $\langle \mathbf{k}_\perp \rangle$ at the vortex center may be shown to vanish over a region of radius ϵ in the limit as $\epsilon \rightarrow 0$. Furthermore, the Fourier transform of Eq. (1) vanishes as $|\mathbf{k}_\perp| \rightarrow \infty$, and thus, there are no rays having an infinite wave number.
- [11] H. J. Lugt, *Vortex Flow in Nature and Technology* (Wiley & Sons, New York, 1983).
- [12] A. G. White, C. P. Smith, N. R. Heckenberg, H. Rubinzstein-Dunlop, R. McDuff, C. O. Weiss, and Chr. Tamm, *J. Mod. Opt.* **38**, 2531–2541 (1991).
- [13] F. S. Roux, *J. Opt. Soc. Am. B* **12**, 1215–1221 (1995).
- [14] N. B. Baranova, B. Ya. Zel'dovich, A. V. Mamaev, N. F. Pilipetsky, and V. V. Shukov, *JETP Lett.* **33**, 195–199 (1983) [*Pis'ma Zh. Eksp. Teor. Fiz.* **33**, 206–210 (1981)].
- [15] B. E. A. Saleh and M. C. Teich, *Fundamentals of Photonics*, edited by J. W. Goodman, Wiley Series in Pure and Applied Optics (John Wiley & Sons, New York, 1991).
- [16] V. Yu. Bazhenov, M. V. Vasnetsov, and M. S. Soskin, *JETP Lett.* **52**, 429–431 (1990) [*Pis'ma Zh. Eksp. Teor. Fiz.* **52**, 1037–1039 (1990)].
- [17] C. T. Law and G. A. Swartzlander, Jr., *Chaos Solitons Fractals* **4**, 1759–1766 (1994).